

acid is fast enough to generate measurable quantities of D-aspartic acid in metabolically stable proteins during the human life-span. D-Aspartyl residues accumulate in enamel (10) and dentin (11) proteins at a rate of 0.1 percent per year, whereas in the lens nucleus the rate is 0.14 percent per year (12).

On the basis of the extent of racemization in a tooth, an age can be calculated for a living individual. With dentin analyses, the racemization age can be expected to fall within ± 10 percent (± 2 standard deviations) of the individual's actual age (11).

An application of interest to physical anthropologists, paleopathologists, and those involved in forensic medicine would be the estimation of the age at death for human skeletal remains. If death occurred in the recent past or if the burial environment is relatively cool, the amount of postmortem racemization is negligible. The D/L Asp ratio in tooth protein therefore reflects the chronological age of the individual (13).

An opportunity for demonstrating this application is provided by the Eskimo cadaver. As a result of accidental inhumation 1600 years ago, this woman's body was well preserved in frozen soils. Racemization analysis of dentin [according to the procedures described in (11)] from a first upper premolar yields a D/L Asp ratio of 0.053. Using the equation (11)

$$\ln(1 + D/L) = 7.87 (\pm 0.39) \times 10^{-4} \text{ yr}^{-1} t + 0.014$$

We calculated age (t) of 48 (± 5) years for the premolar. Five years is added to this age in order to correct for the age of the tooth. The age of the Eskimo woman at the time of death was thus 53 (± 5) years. The racemization age compares very closely with the two earlier estimates based on morphological features.

There are several implications of the reported and earlier (10-12) findings. The amino acid racemization technique may be of practical importance to gerontologists interested in purportedly longevous populations in Ecuador, Hunza, and Russia. Wildlife biologists could also use the technique to construct age profiles for natural populations of large mammals such as whales or dolphins (14) or non-human primates. Very slow rates of turnover in human proteins could potentially be measured (10). If racemization proves to be a widespread phenomenon in structural proteins, it may actually play some role in the aging process of long-lived mammals (15).

The application of the racemization method illustrates that, when available,

multiple approaches are useful in solving paleopathologic problems. Specimens from such unique finds as mummies should be preserved, since techniques will undoubtedly be developed that will lead to the derivation of further information. Finally, studies of this and other Alaskan (16), Egyptian (17), and Peruvian (18) mummies amply demonstrate the value of a collaborative investigation by teams of anthropologists, pathologists, radiologists, biochemists, and other specialists.

PATRICIA M. MASTERS

*Scripps Institution of Oceanography,
University of California, San Diego,
La Jolla 92093*

MICHAEL R. ZIMMERMAN

*Departments of Pathology and
Anthropology, University of Michigan,
Ann Arbor 48109*

References and Notes

1. M. R. Zimmerman and G. S. Smith, *Bull. N.Y. Acad. Med.* **51**, 828 (1975).
2. B. Lawn, *Radiocarbon* **17**, 207 (1975).
3. K. Birket-Smith, *The Eskimos* (Methuen, London, ed. 2, 1959).
4. H. B. Collins, Jr., *Smithson. Misc. Collect.* **96** (No. 1), 82 (1937).
5. G. S. Smith and M. R. Zimmerman, *Am. Antiq.* **40**, 434 (1975).
6. S. D. Stout and S. L. Teitelbaum, *Calif. Tissue Res.* **21**, 163 (1976).
7. J. L. Bada, B. P. Luyendyk, J. B. Maynard, *Science* **170**, 730 (1970); R. M. Mitterer, *Geology* **2**, 425 (1974).
8. J. L. Bada and R. Protsch, *Proc. Natl. Acad. Sci. U.S.A.* **70**, 1331 (1973); J. L. Bada *et al.*, *ibid.* **71**, 914 (1974).
9. J. L. Bada, K. A. Kvenvolden, E. Peterson, *Nature (London)* **245**, 308 (1973); J. L. Bada and P. M. Helfman, *World Archaeol.* **7**, 160 (1975).
10. P. M. Helfman and J. L. Bada, *Proc. Natl. Acad. Sci. U.S.A.* **72**, 2891 (1975).
11. ———, *Nature (London)* **262**, 279 (1976).
12. P. M. Masters, J. L. Bada, J. S. Zigler, Jr., *ibid.* **268**, 71 (1977).
13. P. M. Masters and J. L. Bada, paper presented at a meeting of the American Association of Physical Anthropologists, Seattle, April 1977; paper presented at a meeting of the American Chemical Society, Chicago, September 1977; *Adv. Chem. Ser.*, in press.
14. J. L. Bada, S. B. Brown, P. M. Masters, unpublished results.
15. P. M. Helfman, J. L. Bada, M.-Y. Shou, *Gerontology* **23**, 419 (1977).
16. M. R. Zimmerman and R. H. Tedford, *Science* **194**, 183 (1976); M. R. Zimmerman, G. W. Yeatman, H. Sprinz, W. P. Titterington, *Bull. N.Y. Acad. Med.* **47**, 80 (1973).
17. G. D. Hart, A. Cockburn, N. B. Millet, J. W. Scott, *Can. Med. Assoc. J.* **117**, 463 (1977); A. Cockburn, R. A. Barraco, T. A. Reyman, W. H. Peck, *Science* **187**, 1155 (1975).
18. M. J. Allison, Ed., *Med. Coll. Va. Q.* **12**, 42 (1976).
19. This work was supported by NSF grant EAR 77-14490 and NIH grant PHSAG0063801 to J. L. Bada.

14 February 1978; revised 25 April 1978

Deimos Encounter by Viking: Preliminary Imaging Results

Abstract. Recent close flybys of Deimos by Viking revealed a smooth-appearing surface void of grooves. Higher-resolution pictures showed that the surface was actually covered with craters but that a regolith filled the smaller craters, giving the smooth appearance. The surface was also covered with boulders and bright streak-like markings analogous to base-surge or ejecta cloud deposits.

During October 1977, the orbit of Viking Orbiter-2 (VO-2) was changed to yield five close flybys of Deimos, the outer moon of Mars, all within 1000 km. An orbital commensurability between VO-2 and Deimos of 5 to 4 was achieved when the orbital period of VO-2 was

changed to 24.2 hours. Since the orbital period of Deimos is 30.3 hours, close encounters occurred every 5 days beginning on 5 October 1977. The closest flyby at 33 km (26 km from the surface) took place on 15 October 1977. The sequence of Deimos encounters was ended

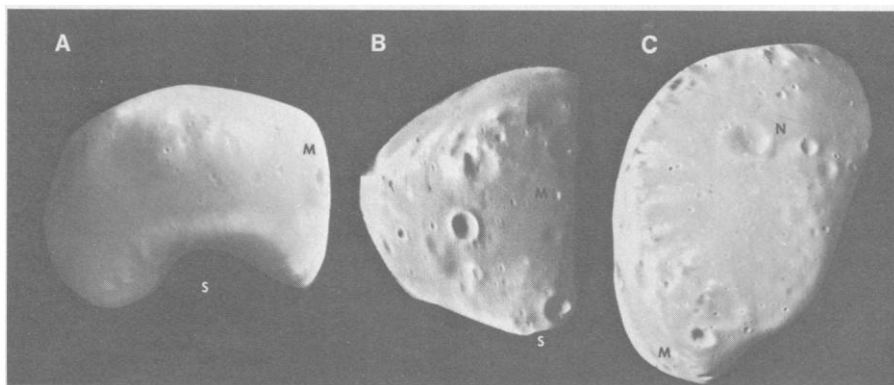


Fig. 1. Deimos viewed at three different perspectives at distances of (A) 1400 km, (B) 1900 km, and (C) 500 km. The illuminated areas are approximately 9 by 14 km with the sub-Mars point (M) and the north (N) and south (S) poles indicated. Even though there is a difference in resolution of a factor of 3 to 4 in these pictures, no significant increase in smaller features is revealed in (C). The apparent absence of craters smaller than 100 m in these pictures (pictures 413B09, 391B05, and 428B07) was found to be misleading.

late in October by an orbit maneuver which brought VO-2 back into an orbit suited for martian observations.

Low-resolution (100- to 200-m) Mariner 9 and Viking images (Fig. 1) showed that, unlike the surface of Phobos, the inner moon of Mars, Deimos is covered with patches having high albedo and appears to be much smoother than the inner satellite. The surface smoothness was puzzling since crater counts indicated that Phobos and Deimos have equal surface densities of impact craters, at least for craters larger than 500 m (*1*).

The very-high-resolution images (Fig. 2) obtained by VO-2 during the October close encounter have resolved this puzzle and have provided convincing information about the nature of these bright patches. The bright patches appear to be deposits of fine-grained material (possibly ejecta) which in several areas partially fill in impact craters, thus accounting for the relatively smooth appearance of the outer martian satellite. Similar bright patches do not occur on Phobos, nor is there any comparably strong evidence of crater-filling on the inner satellite.

Using low-resolution Mariner 9 data, Noland and Veverka (*2*) demonstrated that the bright patches on Deimos have a normal albedo about 30 percent higher than the surroundings but have a phase function essentially the same as that of the surroundings. Thus these bright patches have a texture similar to that of the rest of the Deimos surface—the texture of a fine-grained regolith. Preliminary indications are that there is very little color variation associated with the bright patches.

The high-resolution images also show that the surface of Deimos is littered with numerous isolated, roughly equidimensional features of positive relief (typically ~10 m in size) which have many of the characteristics of ejecta blocks. It appears that these are more common on Deimos than on Phobos, although our best images of Phobos have a coarser resolution than our best images of Deimos.

If the bright patches and blocks represent ejecta, then it is puzzling why apparently so much of it was retained by such a small satellite and why the process seems to be so much more efficient on Deimos than on Phobos. It is conceivable that the very close proximity of Phobos to Mars makes it easier for impact ejecta to escape from the inner satellite, but the mechanics of such a preferential process remain to be worked out.

The high-resolution images also show a new, and as yet unexplained, set of sur-

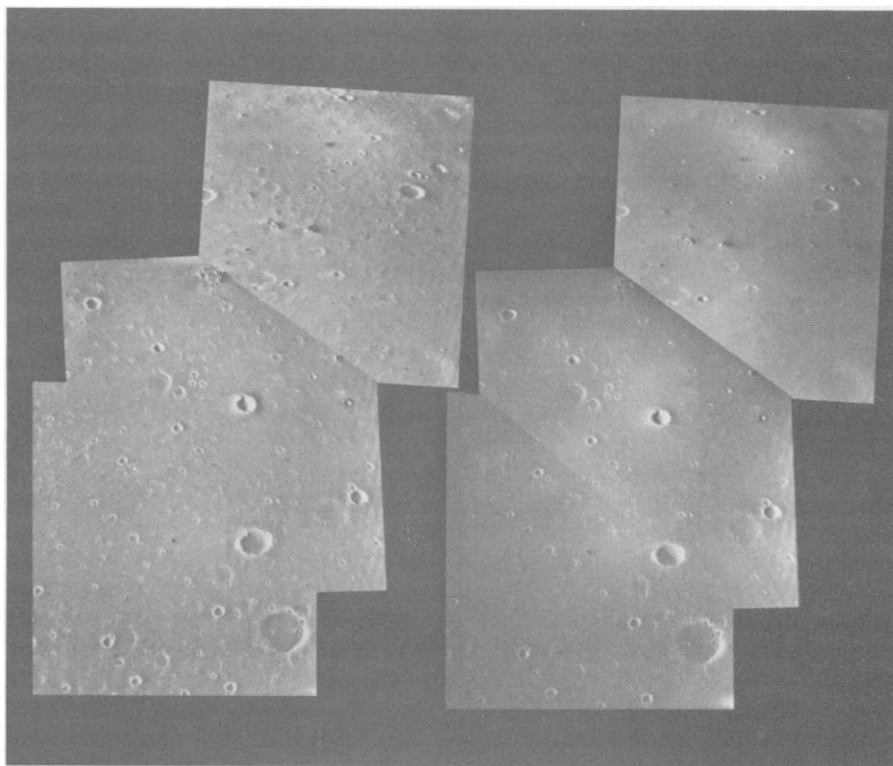


Fig. 2. The surface of Deimos viewed at a range of about 40 km (pictures 423B01 through 423B03). Raw pictures are on the right, and computer-enhanced pictures are on the left. An area covering about 2 by 3 km is seen, which is located in the middle of Fig. 1C on the terminator (north is up). Features as small as 2 m are seen. A heavily cratered surface covered with regolith and strewn with boulders was revealed by these pictures, a completely different view than was obtained from the lower-resolution pictures. Bright streaklike markings are also seen running from the upper right to the lower left.

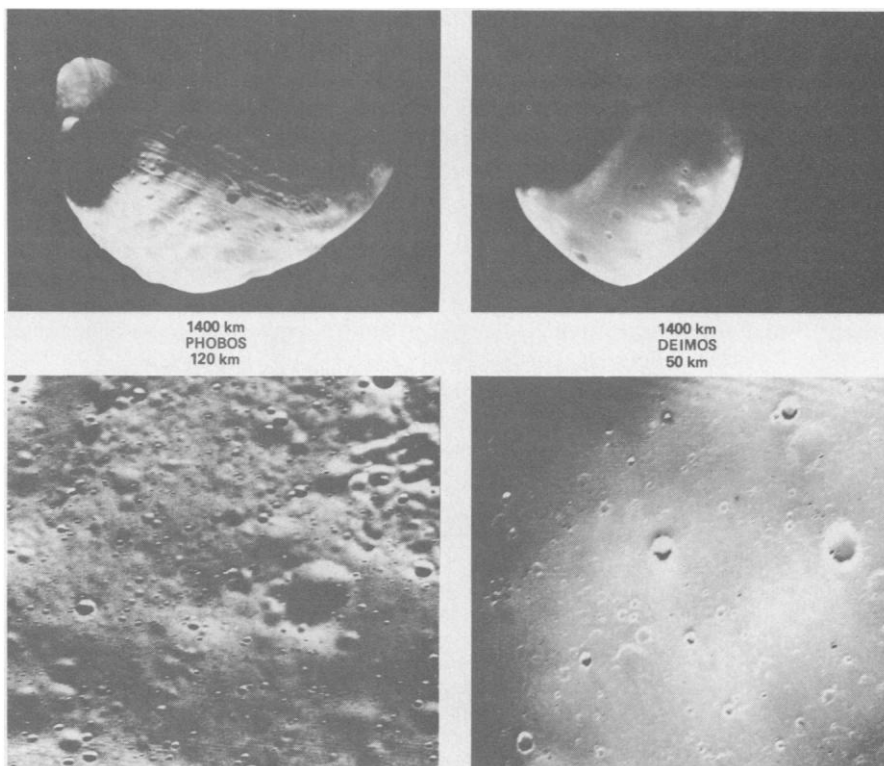


Fig. 3. A comparison between the surfaces of Phobos (left) and Deimos (right). At lower resolution [pictures 315A23 and 413B07 (top)], Deimos appears to be much smoother with significantly fewer craters than Phobos and no grooves. However, higher-resolution pictures [pictures 244B05 and 423B03 (bottom)] show both surfaces to be covered with craters.

face features: bright streaklike markings behind features of positive relief such as crater rims and blocks. These markings appear to be concentrations of fine-grained material (possibly ejecta). It is conceivable that they may be analogous to certain base-surge or ejecta cloud deposits seen on some parts of the lunar surface, but the detailed resemblance is not close.

One of the most exciting results from the October flyby is the evident absence of grooves on Deimos (Fig. 3). From the surface distribution, morphology, and relative age of the grooves on Phobos, Thomas *et al.* (3) have concluded that these grooves are surface expressions of modified fractures associated with the formation of Stickney, the largest (10 km in diameter) crater on Phobos. They also showed that the global pattern and old age of the grooves is inconsistent with the tidal-stretching hypothesis proposed by Soter and Harris (4).

One possible explanation for the absence of grooves on Deimos is that there is no crater large enough on the surface to have caused such global fracturing. In fact, there is no crater larger than about 3 km on the part of Deimos that has been adequately imaged so far (about half the surface area). A large indentation about 10 km in diameter and 2 km deep does dominate the southern hemisphere; but this indentation does not have a crater-like morphology and may be evidence of the fragmentation of Deimos from a once much larger body.

This large indentation has a strong effect on the principal moments of inertia. For Deimos to be in its stable synchronous rotation about Mars, the indentation must be near one of the poles. In fact, it lies close to the south pole of the satellite.

The Viking data showed Deimos to be within 10 km of the position predicted on the basis of Mariner 9 data (5). This prediction error was primarily due to the absence of short-period solar perturbation terms having amplitudes as large as 5 km in the Deimos ephemeris model. The Viking data also suggest that Deimos may be larger than previously believed on the basis of the more limited Mariner 9 data (6). Indications are that the volume is between 1200 and 1500 km³ rather than 1000 km³. One implication of the increased size is that the average geometric albedo may be lower by about 20 percent than previously believed, about 0.05 to 0.06 rather than about 0.07.

Information on the composition of Deimos remains inconclusive. Various data suggest that, although Deimos probably does not have the same composition

as Phobos, it may also consist of some type of carbonaceous material. Tracking data obtained during the October close encounter are currently being processed to derive the mass of Deimos, and additional imagery is being obtained that will make it possible to determine the volume more precisely.

T. C. DUXBURY

*Jet Propulsion Laboratory,
California Institute of Technology,
Pasadena 91103*

J. VEVERKA

*Laboratory for Planetary Studies,
Cornell University,
Ithaca, New York 14853*

References and Notes

1. J. Veverka and T. C. Duxbury, *J. Geophys. Res.* **82**, 4213 (1977).
2. M. Noland and J. Veverka, *Icarus* **30**, 212 (1977).
3. P. Thomas, J. Veverka, T. Duxbury, *Nature (London)*, in press.
4. S. Soter and A. Harris, *ibid.* **268**, 421 (1977).
5. G. H. Born and T. C. Duxbury, *Celestial Mechan.* **12** (No. 1), 77 (1975).
6. T. C. Duxbury, in *Planetary Satellites*, J. Burns, Ed. (Univ. of Arizona Press, Tucson, 1976), pp. 372-381.
7. We thank Drs. D. Elliot, W. Benton, and L. Shigg of the JPL Image Processing Laboratory for enhancing the Viking television pictures. This report is JPL Planetology Publication No. 314-78-17 and presents the results of one phase of research carried out under contract NAS 7-100 and grant NSG-7156 sponsored by the Viking Program Office and Planetary Geology Program Office, NASA Office of Space Science.

17 February 1978; revised 8 May 1978

Earthquake Swarm Along the San Andreas Fault near Palmdale, Southern California, 1976 to 1977

Abstract. *Between November 1976 and November 1977 a swarm of small earthquakes (local magnitude ≤ 3) occurred on or near the San Andreas fault near Palmdale, California. This swarm was the first observed along this section of the San Andreas since cataloging of instrumental data began in 1932. The activity followed partial subsidence of the 35-centimeter vertical crustal uplift known as the Palmdale bulge along this "locked" section of the San Andreas, which last broke in the great (surface-wave magnitude = $8^{1/4}+$) 1857 Fort Tejon earthquake. The swarm events exhibit characteristics previously observed for some foreshock sequences, such as tight clustering of hypocenters and time-dependent rotations of stress axes inferred from focal mechanisms. However, because of our present lack of understanding of the processes that precede earthquake faulting, the implications of the swarm for future large earthquakes on the San Andreas fault are unknown.*

Since 1932, when the California Institute of Technology began to catalog instrumental locations of earthquakes in southern California, the section of the San Andreas fault from the Carrizo Plains to Cajon Pass has been seismically quiet (1, 2). This section of the fault is particularly important because of its known capability for rupture in great earthquakes, such as the 1857 Fort Tejon earthquake of surface-wave magnitude (M_s) $8^{1/4}+$ (3). Seismic quiescence was maintained between 1959 and 1974 during a vertical crustal uplift, the Palmdale bulge (4), which reached a maximum of 35 cm along the southern half of the 1857 rupture zone near Palmdale, California (Fig. 1).

Between mid-1974 and mid-1976 the uplift partially subsided, with an elevation decrease of 17 cm near Palmdale (5). In November 1976 an increase in the number of small earthquakes, of local magnitude (M_L) between 2.0 and 3.0, began in the Palmdale area, near Juniper Hills to the southeast and Lake Hughes to the northwest (Fig. 1). In the year that followed, 1 November 1976 to 1 November 1977, the number of earthquakes with $M_L \geq 2$ was more than an order of

magnitude greater than the long-term averages for these two areas (Table 1). This sharp increase in seismicity, however, does not represent a significant increase in strain energy release, since the recent events are all of small magnitude ($M_L \leq 3.0$) and three earthquakes of $M_L \geq 4.0$ occurred in the Juniper Hills and Lake Hughes regions during the period 1932 to 1976 (1, 2). The relocated epicenter for the largest of these ($M_L = 5.0$, 23 August 1952) lies 2 to 8 km southwest of the San Andreas fault about halfway between Lake Hughes and Juniper Hills (6).

The increase in seismicity extends down to $M_L \approx 0$; this fact has been demonstrated by repeating the extensive 1965 microearthquake surveys of Brune and Allen (7), which established the quiescence of this region down to the smallest detectable earthquake thresholds (8). Seven movable seismographic trailers were installed to supplement existing coverage in the Lake Hughes area for 38 days in February and March 1976 (9). A rate of 1.8 earthquakes per day ($M_L \geq 0$) was determined, compared with 0.1 earthquake per day ($M_L \geq 0$) found between November 1964 and Feb-